















16.8J/cm<sup>2</sup> which is in a good agreement with the threshold for axicon and is similar to the published data [26–29].

Note that the axial fluence produced by the axicon and lens varies by a factor of ~10 over the breakdown region, leading to significant widening of the distal end of the bubble, as observed in the experiment.

Transmission mask that modifies incident Gaussian beam and produces more uniform axial intensity distribution can be designed either by examining the integral in Eq. (1) or, much simpler, by applying the stationary-phase analysis [30]. In order to calculate the axial intensity using this approach we need to know the phase  $\psi$  and the corresponding radial stationary point  $\rho_c$ :

$$\psi(r, z) = \frac{r^2}{2z} - r \sin \theta - \frac{r^2}{2f} \quad (3)$$

$$\rho_c = \frac{fz \sin \theta}{f - z} \quad (4)$$

For the field amplitude transmission function  $t(r)$  of the mask (related to the intensity transmission function  $T(r) = t^2(r)$ ), the axial intensity distribution becomes [30]:

$$\begin{aligned} I_{axial}(z) &= \frac{2E}{\pi w^2} \frac{k^2}{z^2} \exp(-2\rho_c^2/w^2) \left[ \frac{2\pi}{k\psi^{(2)}(\rho_c, z)} \right] \rho_c^2 T(\rho_c) \\ &= \frac{4E}{w^2} \frac{kzf^3 \sin^2 \theta}{(f - z)^3} \exp\left[-\frac{2(fz \sin \theta)^2}{w^2(f - z)^2}\right] T\left(\frac{fz \sin \theta}{f - z}\right). \end{aligned} \quad (5)$$

Since the incident energy at every radial position is focused into its own location on the axis, the breakdown is formed by an annular part of the beam between radii  $r_{\min}$  and  $R$  where the value of  $r_{\min}$  defines the position of the proximal end of the breakdown zone. In our case the coordinate of the proximal end  $z = 16.6\text{mm}$ , which corresponds to  $r_{\min} = 0.9\text{mm}$ . For  $r > r_{\min}$  the amplitude transmission function  $T(r)$  is found from (5) by requesting  $I_{axial}(z) = \text{const}$ :

$$T(r) = \left( \frac{r_{\min} + f \sin \theta}{r + f \sin \theta} \right)^2 \frac{r_{\min}}{r} \exp\left[ \frac{2r^2}{w^2} - \frac{2r_{\min}^2}{w^2} \right], \quad r_{\min} < r < R, \quad (6)$$

The transmission of the central area of the mask ( $r < r_{\min}$ ) can vary. Making it 100% opaque would minimize the overall sample exposure, however, the sharp edge at  $r = r_{\min}$  results in highly oscillatory axial intensity. Making this area transparent, i.e. setting  $T(r) = 1$  for  $r < r_{\min}$ , eliminates such oscillations, but slightly increases the sample exposure. This increase is not significant due to small size of this zone:  $(r_{\min}/w)^2 = 0.05$ . To further decrease the sample exposure while avoiding oscillations in the focal zone, transmission in this area can be gradually increased with radius from 0 in the center to 1 at  $r_{\min}$ .

The intensity transmission function  $T(r)$  defined by Eq. (6) is shown in Fig. 6b. Since stationary-phase analysis does not account for aperture edges it was deemed necessary to verify the performance of such mask by direct numerical calculation of the diffraction integral (Fig. 6a, blue curve). The effect of sharp edge of the axicon aperture is indeed present in the form of rapid oscillations of the intensity distribution, and can be in principle minimized by appropriate apodization. The maximum variation of the axial intensity due to the oscillations did not exceed 40% of the breakdown threshold (blue line in Fig. 6a) – much less than the factor of 10 that was obtained with the original (unmasked) beam (green line in Fig. 6a).

To evaluate the width of the breakdown zone we calculated radial intensity distribution in the focal area close to the region of maximum intensity (Fig. 7). This intensity distribution consists of the strong central peak with full width at half-maximum (FWHM) of  $\sim 2\mu\text{m}$  and side lobes, which do not exceed  $\sim 15\%$  of the central peak intensity. Since transmission mask allows one to keep intensity variations along the breakdown region within 40%, the width of



the breakdown region in the masked beam is limited to the  $\sim 2\mu\text{m}$  wide central peak. Therefore, the aspect ratio of the breakdown zone (of length 1.1mm) is  $\sim 550:1$ . A Gaussian beam with the same FWHM would have confocal parameter of  $\sim 23\mu\text{m}$ , and produce breakdown zone of the similar length. This length is almost a factor of 50 shorter than the length of the breakdown zone achieved with the beam produced by an axicon-lens combination.

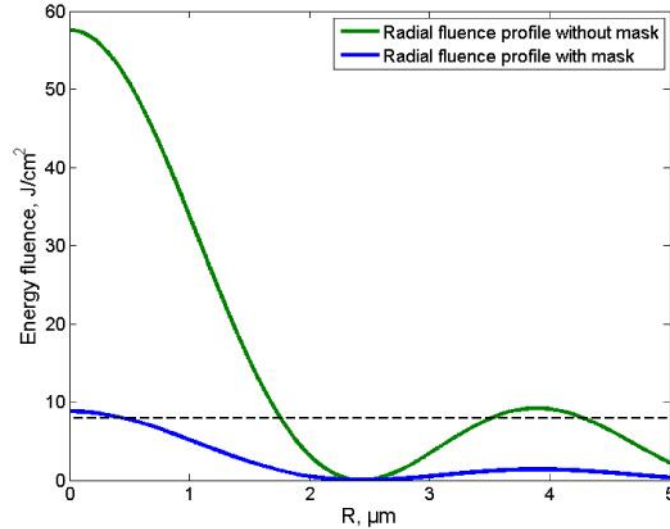


Fig. 7. Radial fluence profile calculated by formula (1) at  $z = 18\text{mm}$  without (green) and with the mask (blue). Dashed line indicates the estimated breakdown threshold of  $8\text{J}/\text{cm}^2$ .

We have tested the computed mask profile experimentally and found that resulting cavitation bubble had the same axial extent but much more uniform width over its length, compared to the unmasked system (Fig. 8). Laser pulse energy in front of the mask was  $270\mu\text{J}$ , corresponding to  $65\mu\text{J}$  transmitted to the sample. This result demonstrates improvement in uniformity of the axial intensity distribution using gradient mask. Taking into account transmission of the clear film (0.6), our theoretical estimate of the pulse energy for the bubble of 1.1mm length was  $65/0.6 = 108\mu\text{J}$ , whereas higher value ( $270\mu\text{J}$ ) was obtained experimentally. This discrepancy may be attributed to several factors. Deviation of the laser beam profile from Gaussian, especially in the periphery where most of the mask modulation is applied, may increase the breakdown threshold. Theoretical estimates also did not account for nonlinear beam propagation, such as self-focusing and plasma filamentation, which could occur in the focal zone.

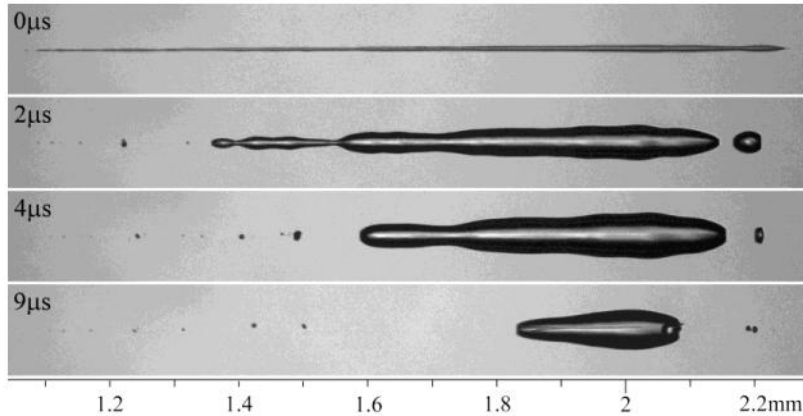


Fig. 8. Dynamics of a bubble produced with the “gradient” mask at less than 100ns, 2 $\mu$ s, 4 $\mu$ s, and 9 $\mu$ s after the laser pulse. Compared to the unmasked beam, this bubble is narrower, more uniform, and has shorter lifetime.

Beam profile can be modified using an electronic spatial light modulator (e.g. LC-R, HOLOEYE Photonics AG, Berlin, Germany), allowing for better control over the actual mask transmission [31]. The fast (a few milliseconds) response time of such modulators provides an opportunity to adjust them between laser pulses, based on a feedback system, which could facilitate more exact control of the shape and the size of the breakdown region.

Inherent drawback of the amplitude beam profile modulation is the energy loss, which might be a substantial obstacle for practical implementation of such a system. The phase modulation of the laser beam might be an ultimate solution for creating adjustable breakdown region in the transparent material.

#### 3.4 Energy considerations – cutting efficiency and safety limitations

In sequential cutting with spherical bubbles the spot spacing is typically on the order of a bubble radius  $R_b$  [32], and thus the number of bubbles required for such a cut  $N = L/R_b$ . For example, for  $R = 25\mu\text{m}$  and  $L = 1.1\text{ mm}$ ,  $N = 44$ . The total volume of these bubbles  $V = 4/3\pi R^2 * L$  is similar to that of a cylinder with the same radius  $R_b$  and length  $L$ :  $V = \pi R^2 * L$ . Therefore, the total amount of energy required for cutting a line with a series of spherical bubbles and with a single cylindrical bubble of the same radius are similar (assuming the same energy conversion efficiency for the cylindrical and spherical bubbles).

In ophthalmic applications part of the laser energy that is not absorbed in the focal zone contributes to heating of the retina. If 67 $\mu\text{J}$  is focused into human crystalline lens at  $\text{NA} = 0.1$ , it produces retinal radiant exposure of approximately 800 $\mu\text{J}/\text{cm}^2$  – over two orders of magnitude below the fluence at which retina pigment epithelium cells get damaged by explosive vaporization of melanosomes – 100  $\text{mJ}/\text{cm}^2$  [33–35]. However, to limit the average retinal heating during prolonged exposure by the same level as with a sequential approach, the laser power should be restricted to the same value, and the pulse repetition rate needs to be reduced accordingly. Therefore cutting planar patterns with the same average laser power will result in the same total duration of the procedure, whereas significant gain in speed can be achieved when creating line cuts (e.g. in applications to membrane poration). For both planar and line cutting the main advantage of the proposed approach is the ability to produce almost instantaneous (within the pulse duration) axial incision without scanning.

#### 4. Conclusions

We have demonstrated highly elongated optical breakdown in water with aspect ratio over 550:1 by focusing laser beam with a combination of an axicon and a lens. Modifying radial intensity distribution of the incident laser beam with the amplitude masks improved homogeneity of the 1mm long linear breakdown zone and allowed for controlling its length

and axial position with 0.1mm accuracy. Axial homogeneity has been improved by a factor of 7, compared to unmasked beam, and did not exceed variation of 40% along the 1.1 mm length of the breakdown zone. Electronic amplitude and phase spatial light modulators may allow for further perfection of the beam profile and for adjustment of the axial position of the dielectric breakdown zone without moving optical elements.

#### **Acknowledgment**

This work was supported by U. S. Air Force Office of Scientific Research (AFOSR) (grant FA9550-04-1-0075).